

Electrochemical Oxidation of $W(CO)_4(LL)$: Generation, Characterization and Reactivity of $[W(CO)_4(LL)]^+$; (LL = α -diimine ligands)

John P. Bullock,^{*a} Chong-Yong Lee,^b Brian Hagan,^a Humair Madhani,^a John Ulrich^a

Contribution from:

- a. Division of Natural Science and Mathematics, Bennington College, Bennington, Vermont 05201, USA
- b. Australian Research Council Centre of Excellence for Electromaterials Science, Intelligent Polymer Research Institute, AIIM, University of Wollongong, Innovation Campus, Wollongong, New South Wales, 2522, Australia

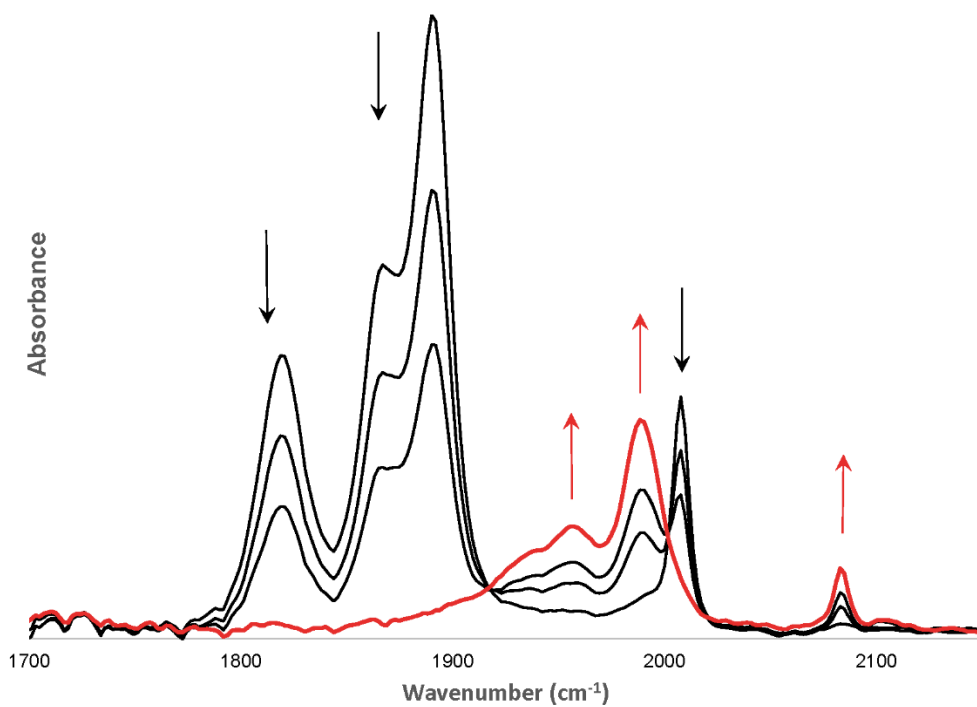


Figure SI-1: Changes in infrared spectra of the carbonyl region during room temperature thin-layer bulk electrolysis of $W(CO)_4(bcp)$, **1g**; arrows indicate the direction of change for the peaks heights. Black traces are experimental data collected while isosbestic behavior was followed; the red trace is the infrared spectrum of **1g+** as calculated from the spectral changes observed before isosbestic behavior was lost.

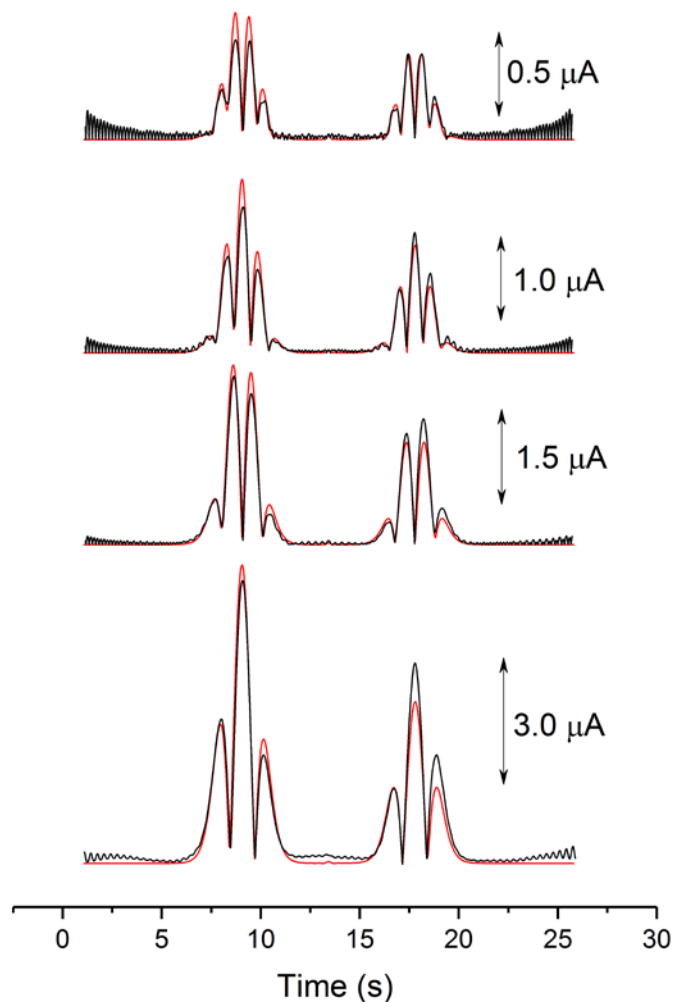


Figure SI-2. Optimized fit of ac voltammetric response for the oxidation of **1a** coupled to simultaneous disproportionation and first-order decarbonylation. Third (bottom row) through sixth (top row) harmonics of large amplitude ac voltammetry results of 0.28 mM **1a** (black traces); red traces show optimized fits. The switching time in each experiment was 13.4 s; peaks observed at earlier times correspond to those occurring during the anodic sweep, those at longer time are from the cathodic sweep. Experimental parameters are: scan rate = 0.0894 V s⁻¹, electrode area = 0.071 cm², ac amplitude, $\Delta E = 0.1$ V, frequency = 13.49 Hz. Simulation parameters: diffusion coefficient = 1.2×10^{-5} cm² s⁻¹, $k^{\circ} = 0.25$ cm s⁻¹, and the homogeneous rate constants (see Scheme 1) $k_{disp} = 400$ M⁻¹ s⁻¹, $k_{first\ order} = 0.2$ s⁻¹, uncompensated resistance = 210 Ω . We attribute the deviations from the observed data to be a result of the exclusion of any equilibrium reactions involving electrogenerated **1a**⁺.

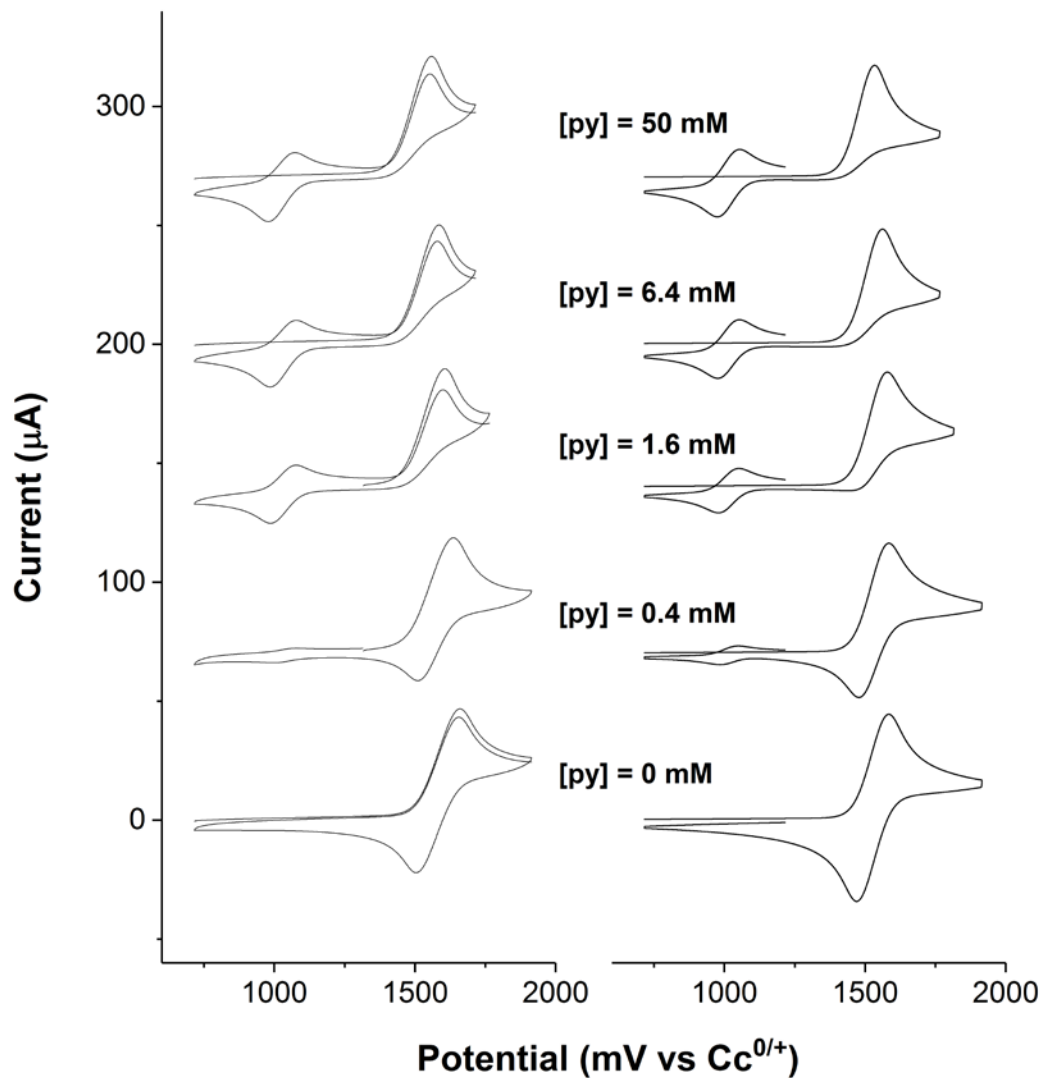


Figure SI-3. Left: Cyclic voltammograms of 1.4 mM **1b** at 0.25 V s^{-1} in the presence of pyridine at the concentrations indicated. Right: Simulations of the voltammograms obtained using the mechanism shown in Scheme 1 with the following rate constants: $k_1 = 2 \times 10^4 \text{ M}^{-1} \text{ s}^{-1}$, $k_{-1} = 1 \times 10^5 \text{ M}^{-1} \text{ s}^{-1}$, $k_2 = 0.10 \text{ s}^{-1}$, $k_3 = 0.20 \text{ s}^{-1}$, $k_4 = 5 \times 10^3 \text{ M}^{-1} \text{ s}^{-1}$, $k_{-4} = 0.1 \text{ s}^{-1}$, $k_5 = 0.35 \text{ s}^{-1}$, $k_6 = 3 \times 10^3 \text{ M}^{-1} \text{ s}^{-1}$. Potentials are in mV relative to $\text{Cc}^{0/+}$.

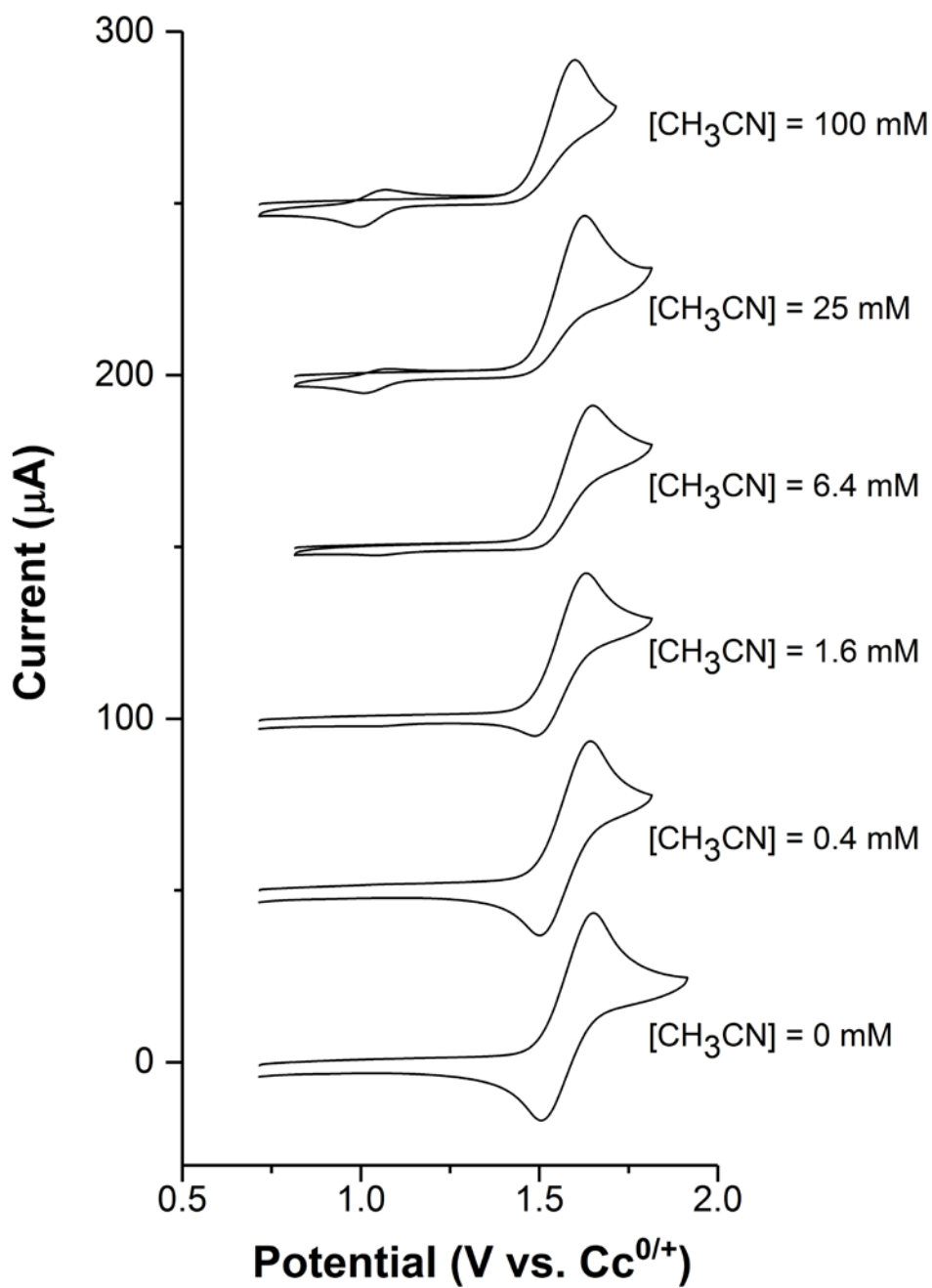


Figure SI-4. Cyclic voltammograms of 1.4 mM **1b** at 0.25 V s⁻¹ in the presence of acetonitrile at the concentrations indicated. Potentials are in mV relative to Cc^{0/+}.